First Lateral Contact Probing of 55-μm Fine Pitch Micro-Bumps

Chang-Keun Kim, Yong-Hoon Yoon, Donguk Kwon, Seunghwan Kim, Gun-Wook Yoon, Min Woo Rhee, Jinyeong Yun, Inkyu Park, and Jun-Bo Yoon, *Member, IEEE*

***Abstract*— Probing micro-bumps for pre-bond testing is an essential process to check for a known good die. In recent technologies, micro-bumps such those used in 3-D-IC are too small and dense, which gives the probing a new challenge. Moreover, developers are concerned that the tip ends of the micro-bumps are mechanically damaged during the pre-bond testing, which is detrimental for the post-process IC assembly. Thus, many low damage probing solutions have been developed, but they still inevitably damage the tip end of the micro-bumps when the conventional probing method, vertical contact, is used. In this paper, for the first time, we demonstrate lateral contact probing on 55-μm pitch micro-bumps without any damage to the tip ends. We successfully realized the testing with monolithically fabricated probes by nickel electroplating with a high aspect ratio photoresist mold. The measured fatigue life of the fabricated probes was at least100 000 cycles. Furthermore, the measured current carrying capacity was more than 180 mA. Proving our concept, the contact test results on the micro-bumps showed no damage to the tip end, and the contact resistance was below 1.13 Ω. Finally, the10 000 probes achieved a uniform 55-μm pitch, which ensured the possibility in real testing. [2018-0041]**

***Index Terms*— Electroplated nickel, fine pitch micro-bump, high aspect ratio photoresist (PR) mold, lateral contact probing, microelectromechanical systems (MEMS) probe card.**

I. Introduction

SEMICONDUCTOR technology has marched at the pace of Moore's law and more for the past tens of years [1]. As transistors have very rapidly kept becoming smaller and faster with more powerful integrated circuits (IC), system integrators have barely satisfied the specifications every time.

Manuscript received February 27, 2018; revised July 31, 2018; accepted August 3, 2018. Date of publication September 18, 2018; date of current version November 29, 2018. This work was supported by Samsung Electronics. Subject editor S. Spearing. *(Corresponding authors: Inkyu Park; Jun-Bo Yoon).*

C.-K. Kim, G.-W. Yoon, and J.-B. Yoon are with the School of Electrical Engineering, Korea Advanced Institute of Science and Technology, Daejeon 34141, South Korea (e-mail: cgkim517@kaist.ac.kr; gwyoon@3dmems.kaist.ac.kr; jbyoon@kaist.ac.kr).

Y.-H. Yoon is with Broadcom Ltd., Seoul 06771, South Korea (e-mail: yhyoon@3dmems.kaist.ac.kr).

D. Kwon is with Samsung Electronics Company, Ltd., Hwaseong 18448, South Korea (e-mail: dukwon8158@kaist.ac.kr).

S. Kim and I. Park are with the Department of Mechanical Engineering, Korea Advanced Institute of Science and Technology, Daejeon 34141, South Korea (e-mail: sunghwan1106@kaist.ac.kr; inkyu@kaist.ac.kr).

M. W. Rhee and J. Yun are with the Mechatronics Research and Development Center, Samsung Electronics, Hwaseong 18448, South Korea (e-mail: minwoo.rhee@samsung.com; jinyeong.yun@samsung.com).

Color versions of one or more of the figures in this paper are available online at http://ieeexplore.ieee.org.

Digital Object Identifier 10.1109/JMEMS.2018.2868871

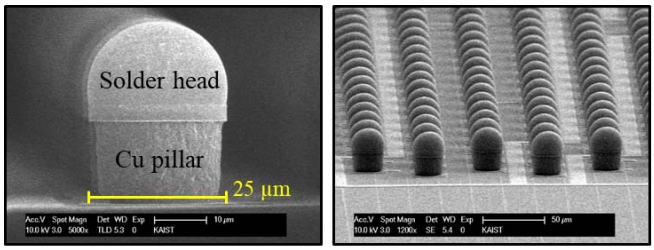

Fig. 1. Geometric view of micro-bumps. (a) A side view of a 25-μm diameter micro-bump consisting of a solder head and a Cu pillar. (b) Micro-bumps in an array of 55-μm pitch.

Previously, there were not many signals to process in a chip, so were the electrodes on a chip. However, as miniaturization of a chip undergoes, more signals needed to be processed. Thus, many more electrodes with scaling had to occupy a chip, and they evolved from a flat structure to convex balls or bumps such as ball grid arrays for dense integration [1], [2]. Eventually, electrodes became *micro-bumps* with a size of several tens of micrometers and a very fine pitch of below 100 micrometers as depicted in the example in Fig. 1. The structure of a micro-bump itself is divided into a head and a pillar as shown in Fig. 1(a). The head is then connected to another IC and is usually made of a solder such as a Sn alloy, and the pillar is made of Cu. This advancement enabled integrators to successfully stack chips vertically following "more than Moore", such as in a 3D-IC stack [1]–[5].

At the same time, there was another industry as busy as the system integration: IC testing. To obtain an acceptable IC yield, performing *pre-bond IC testing* is essential as depicted in Fig. 2(a)-(b). Thus, when a new IC comes out, a new IC testing technology must follow. For the testing, an interface with electrical probes called a probe card contacts electrodes on a IC chip and allows the chip be connected to a tester to exchange signals to check whether it is a known good die (KGD) [6].

Therefore, as expected, though micro-bumps improved IC technology significantly, pre-bond IC testing created another problem. As mentioned, micro-bump arrays of a chip are so small and dense that probe arrays of a probe card are very difficult to catch up the development of micro-bumps. First of all, creating a fine pitch probe array to contact one-to-one with thousands of a fine pitch micro-bump array is a big challenge [7], [8]. Particularly, a probe needs sufficiently flexible structures because with a rigid probe, the tip end of

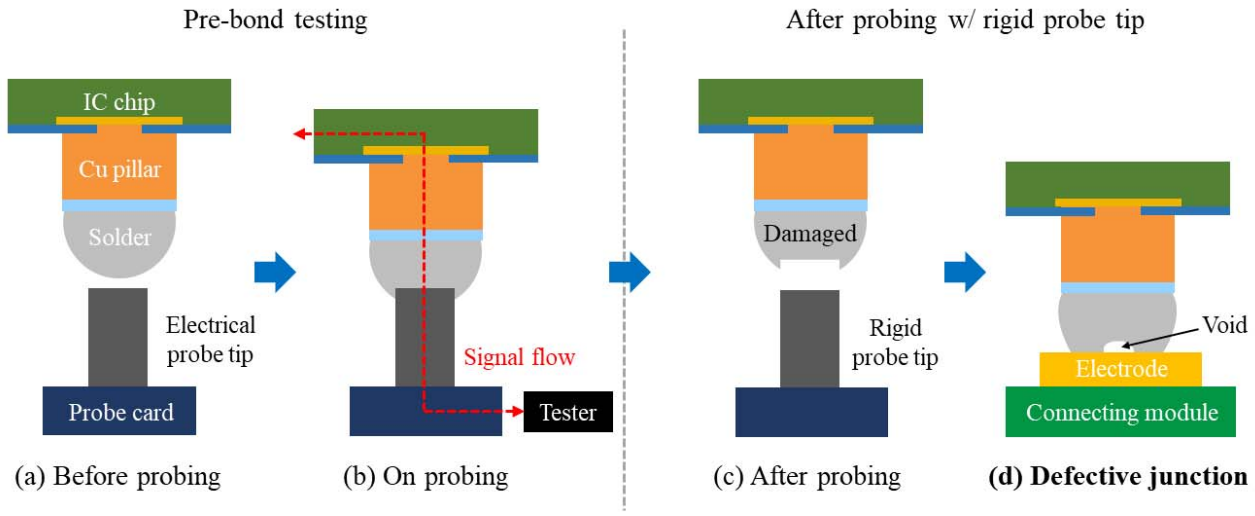

Fig. 2. Conceptual illustration of the pre-bond IC testing of a micro-bump and the issue of a rigid probe tip contacting a micro-bump. (a) When the electrical probe tip contacts the micro-bump, (b) the electrical path is made and signals are exchanged between the IC chip and the tester. (c) If the micro-bump is probed with a rigid probe tip, as it contacts the weak solder vertically the tip end of the weak solder is damaged. (d) This issue creates an incomplete and a defective junction between chips at the IC assembly stage after the pre-bond IC testing. Also, the void accelerates degrading the mean-time-to-failure of the junction.

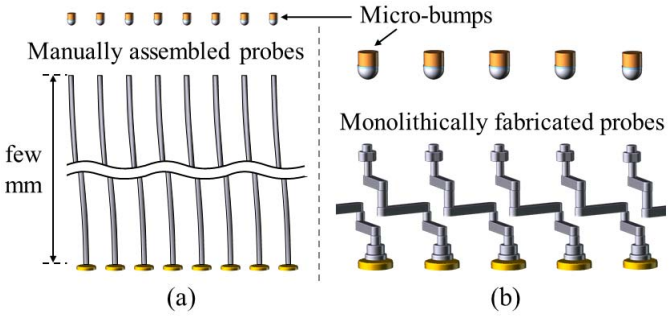

Fig. 3. 3D illustration of two most common existing types of probes for testing fine pitch micro-bumps. (a) Very long and thin rods as probes such as 30 μm in diameter and 5 mm in length assembled vertically and manually one-by-one on the substrate [17]. (b) Monolithically fabricated MEMS probes which need complicated processes to be highly flexible as previous vertical probes [25].

the weak solder of the micro-bump is badly damaged after the probe-bump contact test as shown in Fig. 2(c). Though the chip and the probe card micro-bump arrays on the chip cannot avoid damage because micro-bump arrays on the chip cannot avoid damage because they must be contacted by probe arrays at once with having the height error of micro-bumps themselves and of the substrate [9]–[11], [14]–[17]. Then, as shown in Fig. 2(d), damage to the tip end of the solder causes problems such as incomplete or defective junctions between ICs in the post-testing stage: IC assembly [12]–[16]. Also, the void accelerates degrading the mean-time-to-failure of the junction due to the current crowding near the junction interface [18], [19]. These issues are very important because even though the chip is well tested as a KGD, the yield is lower due to defects in the IC assembly.

To overcome this issue, probes have been researched broadly to get higher and higher flexibility. Fig. 3(a) shows vertically long, thin rods as probes each 30 μm in diameter and 5 mm in length, fabricated using a microfabrication technique [17]. These probes are fabricated horizontally and then are assembled vertically and manually on the substrate one-by-one, which has the advantage of having large displacement even with very weak force. Though this way of fabricating probes is dominant in the industry, it needs too much time and effort to be made due to its non-automatic assembly, and it is very disadvantageous from an economical point of view. On the other hand, recent technologies with micromachining and MEMS techniques have fabricated monolithic probes in a batch [12]–[15], [20]–[25], as for example that shown in Fig. 3(b). Probes of this type are less flexible than the previous type but have the advantage of being fabricated in batches with monolithic MEMS processes. However, no matter how flexible they are, the tip end of the solder inevitably damages after the probe-bump contact test because these probes in Fig. 3(a) and (b) all vertically contact the micro-bumps in the end. Moreover, in order to minimize the damage, these probes require a very tough process, such as manual assembly or very complicated monolithic MEMS fabrication as mentioned above.

In this paper, we break the existing frameworks of the vertical contact probing and propose a new method, lateral contact probing, which does not damage the tip end of the solder at all, and we demonstrate the electrical contact testing for the first time. At the same time, we present a simple design and a verification of probes for the lateral contact probing which can be fabricated by a monolithic MEMS process. Furthermore, about 10,000 probes are arrayed in a 55-μm pitch in a very uniform structure. Since there is no damage to the tip end of the solder nor is a complex fabrication process required, the proposed method is expected to be employed very widely in the current application fields of MEMS probe cards.

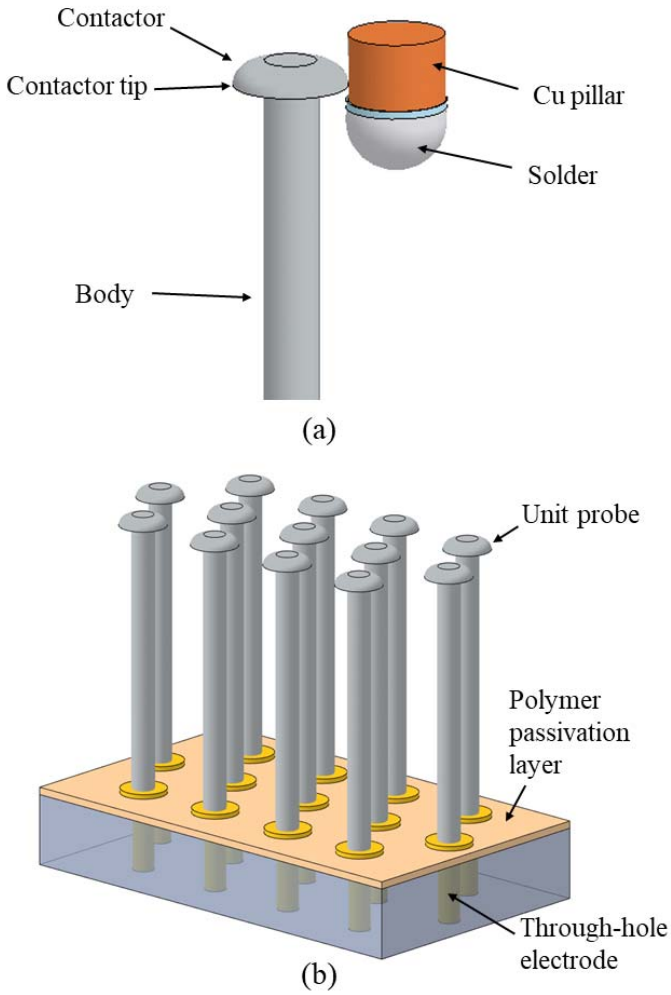

Fig. 4. 3D schematic view of the proposed lateral probing method along with the probes. (a) Lateral contact in the contactor of the probe and the side-wall of the micro-bump. (b) Probes in a fine pitch array are simply mushroom-shaped and monolithically fabricated on the substrate of a probe card.

II. Proposed Concept and Probe Design

Since the electrodes are not flat as in the past and are now three-dimensional (3D) as micro-bumps, we do not need to stick to vertical contact, the traditional probing method. Fig. 4 gives a schematic illustration of the proposed lateral probing concept and mushroom-shaped probes for it. As you can see in Fig. 4(a), the mushroom-shaped probe, consisting of a contactor and a body, does not touch the tip end of the solder, and thus the tip end will not be harmed at any time. Unless the alignment between the probes and micro-bumps is incorrect, the contactor part of the probe only touches the side-wall of the micro-bump. After the contact, the body bends only a few micrometers in a lateral direction as the probe drives towards the micro-bump for better contact. Whereas vertical contact probes need to be highly flexible to overcome the height error of the chip, lateral contact probes do not need to be highly flexible because there is not much error in horizontal alignment compared to the vertical error. Moreover, this method is very insensitive to a height error of the micro-bumps and the substrate because probes and micro-bumps contact each other only in the lateral direction as

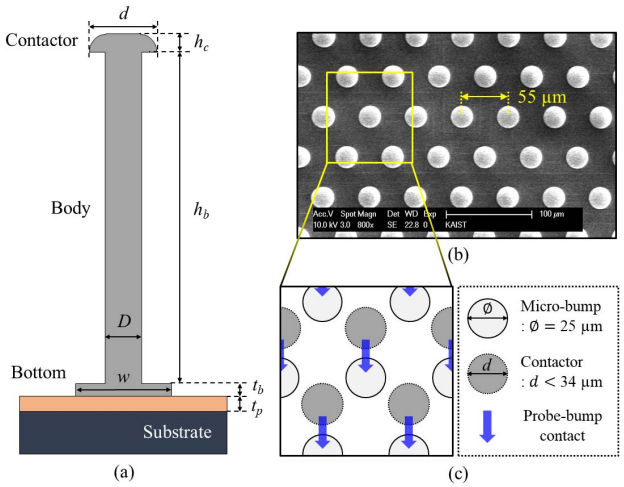

Fig. 5. Geometric parameters of the mushroom-shaped probe in its vertical cross sectional view and its top view with the actual micro-bump array. (a) The probe consists of a contactor, a body with a bottom supporting electrode, and a polymer passivation layer underneath it. (b) SEM image of the actual micro-bump array in top view. (c) Position and possible size of the probes to contact the micro-bumps. The geometrical values are listed in Table I.

TABLE I
Geometric Parameters and Dimensions for the Proposed Probe

Parameters		Symbol	Value (μm)
Contactor	Diameter	d	24 – 34
	Height	h_c	5
Body	Diameter	D	14
	Height	h_b	120
Bottom	Electrode width	w	25
	Electrode thickness	t_b	3
	Polymer layer thickness	t_p	8

described above. Therefore, we can use this lateral probing method with very simply structured probes as shown in Fig. 4(b). These very simple looking probes do not need to be assembled or undergo complicated fabrication processes. As will be described later in the fabrication section, these fine pitch probes are monolithically fabricated with only one layer of a thick PR mold followed by one-step nickel electroplating. Ultimately, with the simpler fabrication process for the probes, we expect better probing results that do not damage the tip end of the micro-bumps.

To design the mushroom-shaped probes for contacting fine pitch micro-bumps laterally, as shown in Fig. 1, we divided the design parameters into the contactor, the body, and the bottom. All the geometric parameters of the designed probe are depicted in Fig. 5(a) as in a vertical cross sectional view of the probe, and their specific values are listed in Table I. We describe the design considerations in the next section.

A. Contactor

Since the contactor touches the side-wall of the micro-bump directly, its shape, material, and size of the contactor needed to be precisely considered. The factors under consideration were contacting direction, contacting property, and compatibility with the micro-bump array. First, as same as the micro-bumps, we applied circular shape in horizontal cross section for the contactor to accommodate all the contact directions. Second, we selected MEMS electroplated nickel, which has generally good electrical contact to the other metals, high corrosion resistance, and economical advantages [26]–[28]. It is widely adopted in actual use in testing micro-bumps [20]–[24]. Also, it is expected that better characteristics will be obtained if Nichrome or rhodium is coated over. Third, to ensure the probe arrays infiltrates safely into the micro-bump arrays as shown in Fig. 5(b)-(c), we determined the diameter of the contactor to be less than about 34 μm considering the size of the micro-bumps, 55-μm pitch, and the horizontal alignment error of 2 μm in maximum, which was provided from the actual industrial site, Samsung Electronics. The minimum size was determined after the body was designed, as described in the next section.

B. Body

The body of the probe must have a bit of flexibility for elastic bending after the contact. Its shape, material, and size of the body were considered as the key factors. Its shape and material were determined as a circular shape and MEMS electroplated nickel for the same reasons as for the contactor above. Then for the size of the body, which directly relates to the flexibility, we looked at how much displacement in the lateral direction would be required for the probe to move after the contact. It was speculated with the actual horizontal alignment error of 2 μm in maximum and an assumption which the contact will form metal-to-metal contact. Thus, we targeted 5 μm for the displacement at least. Furthermore, we had to ensure that the probe could move sufficiently in the elastic region by the target displacement. As depicted in Fig. 6, finite element analysis (FEM) simulation was performed, and the size determination of the body according to the result is shown in Table I. Followed by, considering the size of the body and its pushed displacement, 5 μm in target, the minimum size of the contactor was determined as 24 μm, which is designed not letting the body to touch the head of the micro-bump directly.

C. Bottom

Finally, we considered the bottom electrode and the polymer passivation layer for the alleviation of the stress. The bottom electrode supports the electrical connection between the probes and the through-hole via. It is 3 μm thick and 25 μm wide. We believe it can be optimized in the future work with a real probe card substrate. The polymer passivation layer is a necessary part underneath the probes and protects the whole surface of the probe card. It is usually structured of a permanent polymer, such as polyimide (PI), and has a thickness of about 8 μm or less. Thus, we chose SU-8 for the passivation layer due to its characteristics similar to PI and its ease of fabrication.

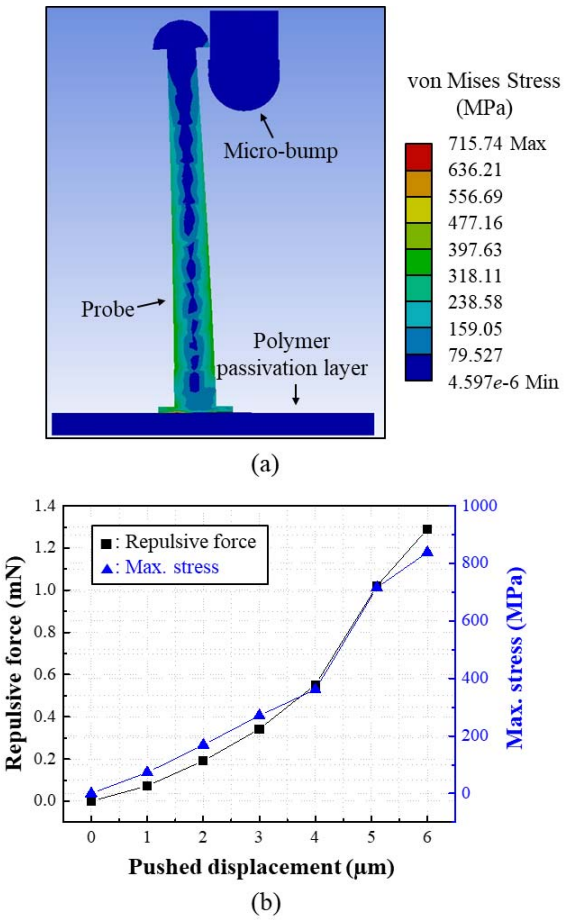

Fig. 6. FEM simulation results to investigate stress distribution by pushing displacement. (a) Viewed by a vertical cross section, von Mises stress distribution over a laterally driven probe by 5 μm after the contact. The overall stress of the structure was found to be about 300 MPa, with the highest stress at very tiny part of the bottom. (b) Repulsive force and maximum stress of the probe by pushed displacement is shown.

Fig. 6 presents the mechanical analysis with the FEM simulation (ANSYS) results of the laterally bending probe after it contacts the micro-bump. The lower body of the simulated model was considered to be wider than the upper body due to the lithographic characteristics of the negative PR in real fabrication. To investigate whether the probe is driven in the elastic region, we checked its von Mises Stress. Since the probe has a circular shape in the horizontal cross section, the bending probe has the highest stress in the center line in the bending direction. The simulation results of 5 μm in its lateral bending direction shows the highest stress as about 300 MPa in the probe body, and it is speculated to be in the elastic region as the yield stress of the electroplated nickel is expected to be about 800 MPa [27]–[29]. However, we can see the highest stress was 715.74 MPa in the legend, but that seems insignificant because it was only a tiny area at the bottom electrode. Moreover, almost no stress was seen in the polymer passivation layer. Also, we checked values

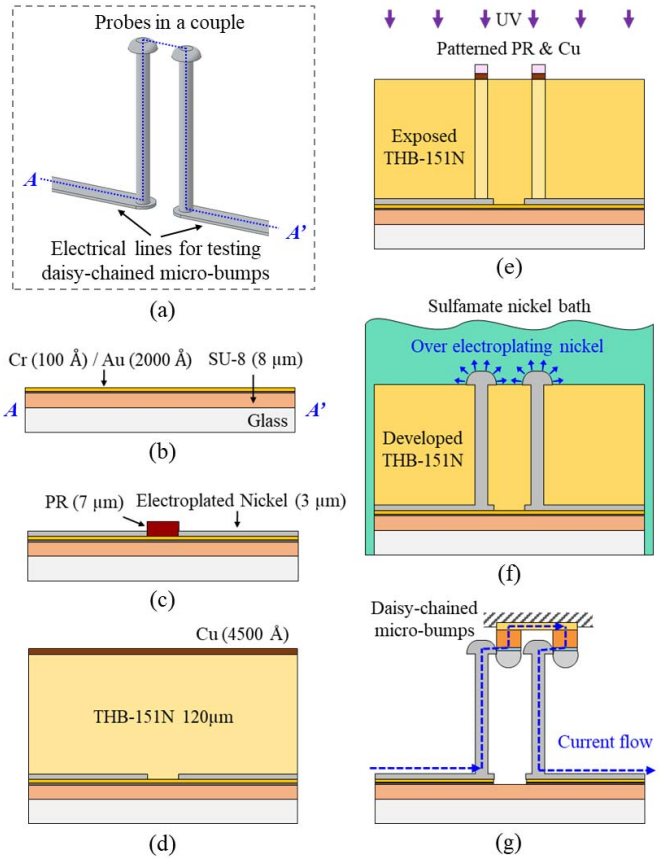

Fig. 7. Fabrication process of the proposed probes for the daisy-chained micro-bumps. (a) 3D schematics of the probes designed in a couple with electrical lines to test daisy-chained micro-bumps. (b) Polymer passivation layer (SU-8) and seed metal layer deposition. (c) Bottom electrode formation by a pre-patterned PR mold. (d) Thickly spin-coated and baked THB-151N and Cu deposition on top of it as for a photo-masking layer. (e) Exposing UV with a pre-patterned Cu layer by a thin PR layer. Development of the PR follows. (f) Within the developed PR mold, nickel is electroplated and overflowed to create the contactor part of the probe. Then, wet etching process of the PR mold and seed metal layers for the electrical isolation of two probes. Appropriate drying follows. (g) Fabricated result with description of measuring the electrical properties of the daisy-chained micro-bumps.

and linear characteristics of the repulsive force by the pushed displacement. These results can be compared later with tested characteristics of the actual probe to verify whether the probe is reasonably fabricated. Throughout all the simulation results, we found that not only the long flexible probe but also the polymer passivation layer plays a very important role, which relieves the overall stress when the probe is pushed in the lateral direction. In conclusion, the designed probe is expected to safely bend 5 μm in the lateral direction with a long fatigue life in the elastic region [30].

III. Fabrication

The proposed probes were fabricated in a pair to test the daisy-chained micro-bumps and the overall fabrication process is described in Fig. 7. The daisy-chained micro-bumps are electrically connected to each other and are not connected to other chips in order to be used for testing purposes only. Therefore, to measure the electrical properties of the daisy-chained micro-bumps, the probes need electrical lines out of them and the current flows as depicted in Fig. 7(a), (g).

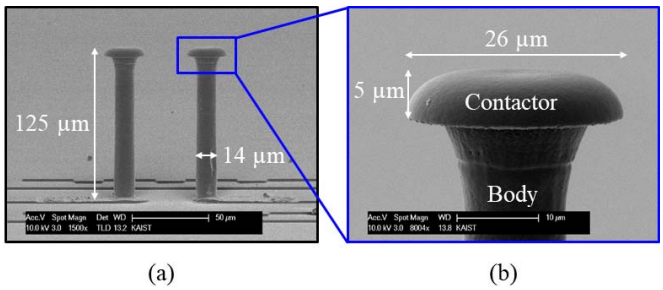

Fig. 8. SEM images of the fabricated probes. (a) The nickel probes and the bottom electrodes are shown as designed. (b) Magnified view of the contactor.

The whole fabrication process only uses two photomasks in total, one for patterning the bottom electrode lines and the other for the mushroom-shaped probes. The main substrate used in our process was a transparent glass wafer due to our see-through electrical testing equipment for aligning the probes and micro-bumps, which will be described later. On a bare glass wafer, the fabrication started with preparing an 8 μm thick SU-8 layer as depicted in Fig. 7(b). Then we thermally evaporated Cr (100 Å) as an adhesion promoter and Au (2000 Å) as the seed metal to electroplate nickel. To fabricate the bottom electrodes as electrical lines, the seed metal was electroplated with nickel about 3 μm thick within a patterned positive PR as shown in Fig. 7(c). After electroplating and etching all the residue of the PR, THB-151N(negative PR, JSR product, Japan) was spin coated as 120 μm thick. Then as shown in Fig. 7(d)-(e), Cu (4500 Å) was thermally evaporated and patterned on top of the THB-151N for an embedded photomask [31]. This is our prior technique that maximizes the resolution of the lithography by removing the space itself between the PR and the photomask. The Cu embedded mask was patterned with wet etching by a patterned thin positive iPR. Using it as a photomask, THB-151N was exposed with an appropriate amount of ultraviolet (UV), and all the Cu embedded mask was removed for the development of the PR. Developing was carried with tens of minutes due to the deep PR mold. Then, the PR mold was rinsed with de-ionized (DI) water thoroughly all the way to the bottom. After that, the PR mold was ready to be electroplated. To obtain good mechanical characteristics of the probes, we used a sulfamate nickel bath to electroplate elastic nickel as determined in the simulation part above. We also electroplated the whole wafer with nickel within the mold and moreover allowed it to overflow out of the mold. Stopping the electroplating at the appropriate time, it naturally created the contactor part of the probe as described in Fig. 7(f). After all the probes were made, the PR mold was s lowly removed in the wet etchant and the seed metal layers were patterned by wet etching for electrical isolation between the probes. Finally, the fabricated probes were ready to contact the micro-bumps, and its images from a scanning electron microscope (SEM) are depicted in Fig. 8. All the parts were well created, and also the body was wider in the lower part as we expected.

IV. Measurement Results

Mechanical and electrical properties of the probe itself were tested to determine its movable displacement and its operating

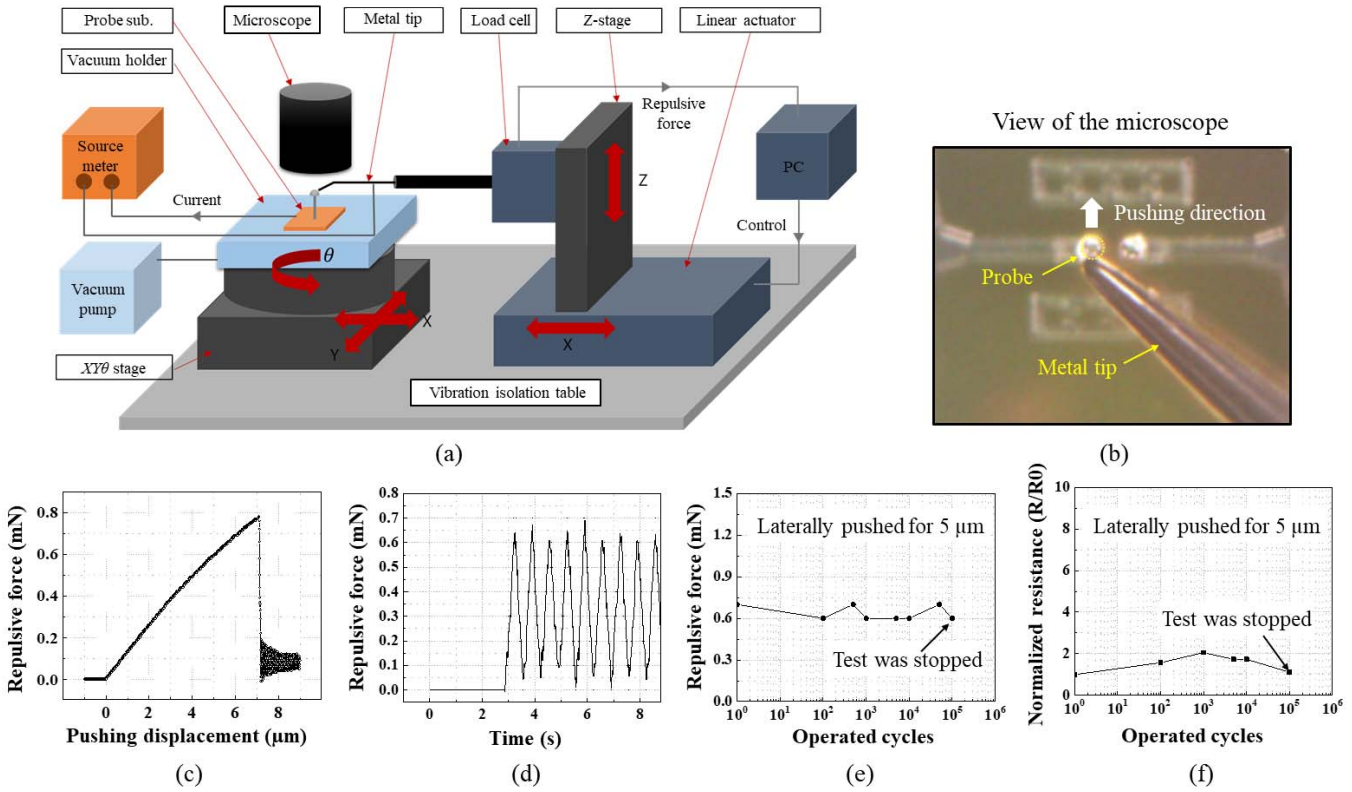

Fig. 9. Characterization of a probe itself. (a) Conceptual illustration of the testing system. The linear actuator can move in units of 100 nm and the load cell can measure the repulsive force in units of 0.1 mN. (b) Actual testing view of the metal tip pushing a probe in the lateral direction. (c) Measured tipping displacement versus repulsive force of a laterally driven probe. It was driven safely as much as 7 μm and then it broke. (d) Measured repulsive force by pushing a probe at a frequency of 1.5 Hz. (e) Measured operating life of a probe by measuring its repulsive force. The repulsive force did not decrease until the test stopped at 100,000 cycles. (f) Here, we define the normalized resistance as the electrical resistance compared to the value of the first contact. The values did not change significantly even after repetitive mimic contact tests.

life cycle. Then, the lateral contact testing of the micro-bumps was evaluated. The detailed characterization follows by.

A. Operating Characteristics of the Probes

First, we investigated the probes for their operating characteristics as evaluated in Fig. 9. The testing system was built on a vibration isolation table and is conceptually described in Fig. 9(a). There is a metal tip on a linear actuator that moves laterally by 100 nm with a load cell which measures the repulsive force by 100 μN when the metal tip pushes the probe held by a vacuum pump. The actuator can be controlled by a connected PC. Looking in the microscope, we could align the metal tip and the probe with controllable stages. As shown in Fig. 9(b), the metal tip and the probe are aligned and the metal tip pushes the probe laterally. As the probe was being pushed, the repulsive force was measured as in Fig. 9(c) and it shows a proportional increment as the pushing displacement increases. It has a spring constant of 0.12 mN/μm, which is very reasonable compared to the result shown in Fig. 6(b). Also, the probe broke down after moving 7 μm eventually. These results tell us that a probe can be driven safely around our target at a displacement of 5 μm as we expected with the FEM simulation result shown in Fig. 6.

After investigating the movable displacement, we then tested the operating life of the probes as shown in Fig. 9(d)-(f). We considered that the repulsive force of the probe would not decrease as long as it was in the elastic region. Fig. 9(d) shows that the repulsive force of the probe pushed 5 μm at a frequency of 1.5 Hz is about 0.6 mN. Furthermore, the measured repulsive force operating up to at least 100,000 cycles is constant as the initial value as shown in Fig. 9(e). This can be explained as the fatigue life of the probe is over 100,000 cycles at least as we expected with the FEM simulation result in Fig. 6 [30]. Though we expected

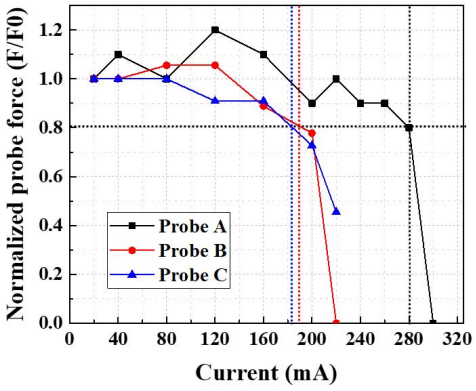

Fig. 10. Measured current-carrying-capacity (CCC) of the probes. The three probes have CCC values at least larger than 180 mA.

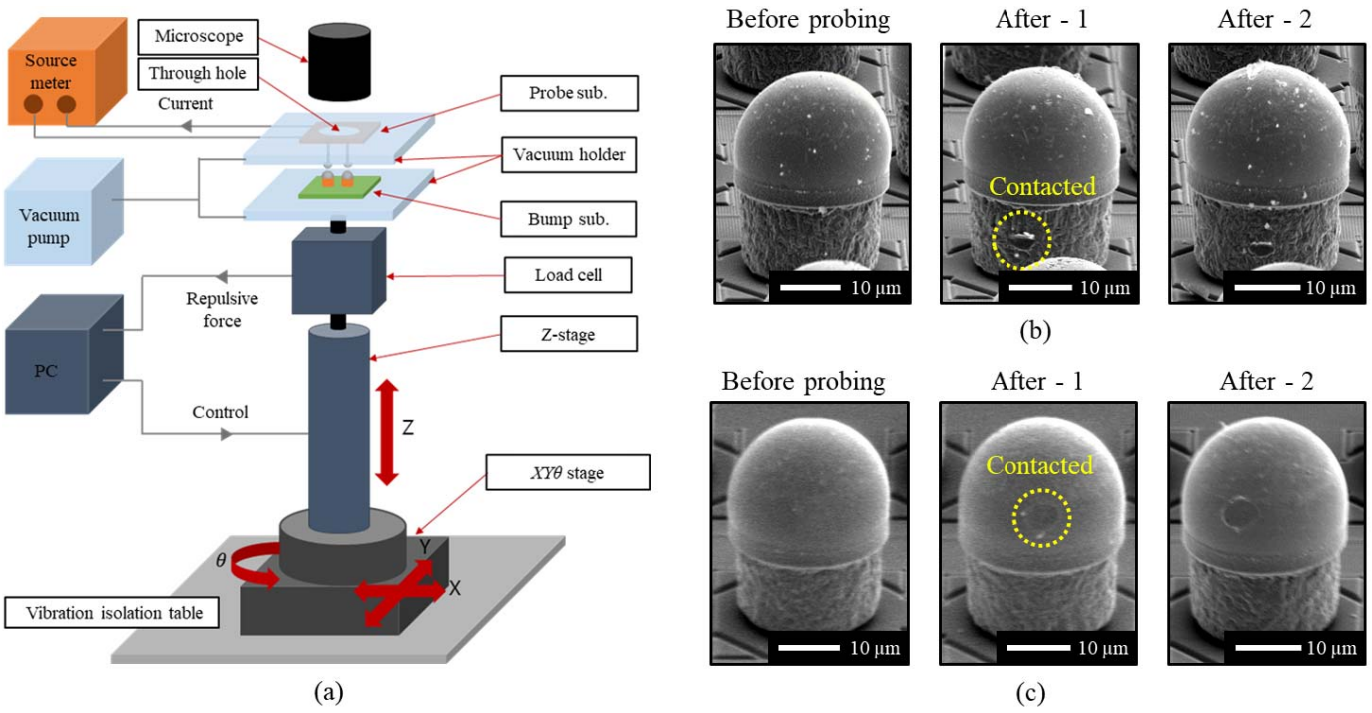

Fig. 11. Contacting the micro-bumps with the probes. (a) Conceptual illustration of the contact testing system. (b) SEM images of before and after the contact on the side-walls of the Cu pillars of two different micro-bumps. No damage on the tip end of the solder is seen. (c) SEM images of before and after the contact on the side-walls of two different solders. As same as in (b), there is no damage on the tip end of the solder.

that the measured repulsive force would be more consistent if a more accurate load cell was used, the result shows a sufficiently constant value. Based on the fact that the contact resistance at the nano-micro scale is mainly dominated by the contact force [32]–[34], we concluded from this result that the contact properties of the probe with the micro-bump will be consistent up to at least 100,000 cycles. Even after pushing another probe repetitively by 5 μm, the electrical resistance of the metal tip to the probe did not change significantly as shown in Fig. 9(f). Although quite different from the actual test of contacting micro-bumps, we have predicted the persistence of electrical characteristics by this mimic contact test here with the metal tip, because it was difficult to measure every new micro-bump for hundreds of thousands of times in our experimental stage. Thus, we speculated that the probe would not be modified either mechanically or electrically.

Additionally, we measured the current carrying capacity (CCC) of the probes as shown in Fig. 10. This property is a critical parameter in the industry to determine the highest current at which a failure occurs by a thermal event such as Joule heating. Among the measuring methods, we chose the ISMI'09 method [35], which is very widely used. The CCC value corresponds to a drop of 20% of the repulsive force of the probe during a continuous current supply, where the current is increased by a given step (here, 40 mA for 120 s). Then the force must be measured after a few minutes to allow cooling down to room temperature. The reduction of the force is mainly due to the Joule heating of the probe, which leads to plastic deformation. Our result in Fig. 10 shows that the tested probes have CCC values larger than 180 mA. Given that the probes are finely pitched at 55 μm, this value is an acceptable result [36].

B. Contacting Micro-Bumps

Since the evaluation of the probes was successful, we conducted contact testing on daisy-chained micro-bumps and successfully demonstrated the lateral contact as shown in Fig. 11. To bring the probe into lateral contact with the micro-bump, another testing system was built on a vibration isolation table, and it is conceptually illustrated in Fig. 11(a). Both the probes' substrate and the micro-bumps' substrate were held still by a vacuum pump facing each other up and down. Then, looking in the microscope, we could see the bumps through the probes' substrate by its transparent glass wafer and align the probes and the micro-bumps with the controllable stage. By moving the stage up by 1 μm and checking the repulsive force of the load cell by 1 mN, we could see whether the two substrates were in contact with each other, and we finished the alignment in a very detailed way. After all, the probes in pairs were driven laterally by a few micrometers and contacted the daisy-chained micro-bumps successfully as shown in Fig. 11(b)-(c). The SEM images show the before contact and the after contact of different micro-bumps. The probing marks on the side-walls of both the Cu pillars and the solder are clearly visible but are not big and deep. Thus, the newly proposed concept of probing the micro-bumps was proved to be efficacious. With this lateral contact probing, there was no probing mark on the tip end of the solder, which is what causes the defective junction at the post-testing stage: IC assembly.

TABLE II
MEASURED CONTACT RESISTANCE

Micro-bump / Contact part	A	B	C	D	E	F
Cu pillar	0.86 Ω	1.13 Ω	0.31 Ω	-	-	-
Solder	-	-	-	0.75 Ω	1.1 Ω	0.88 Ω

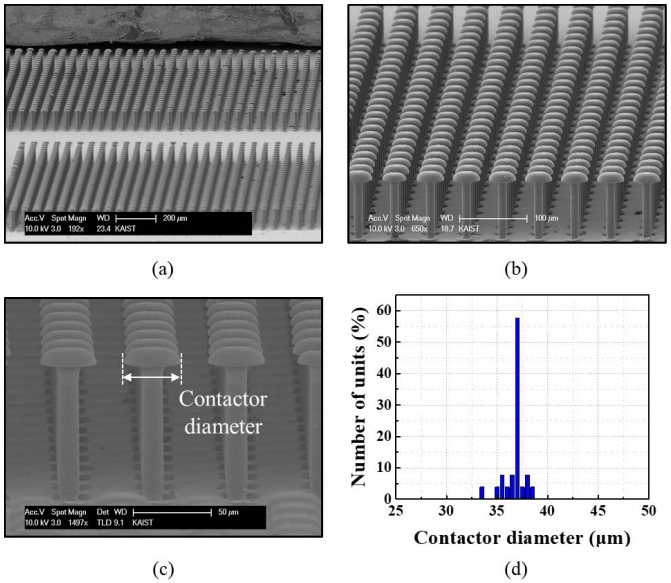

Fig. 12. Fabricated probes in arrays. (a) Thousands of probes are fabricated in arrays. The SEM image is a somewhat zoomed view. (b) More magnified view. (c) Magnified view of a few contactors indicating the contactor diameter in the image. (d) Statistical data of the uniformity of the contactor diameter that supports the possibility of the realization.

In the actual test, the contact by the electrical current flow was as depicted in Fig. 7(g). Since the obtained system resistance value was reproducible, the contact resistance was obtained from all other micro-bumps as listed in Table II by excluding the system resistance at the measured total resistance. Within the contact on the Cu pillar or the solder of the micro-bumps, each value of the contact resistance was near or below 1 Ω. Metal-to-metal contact occurred smoothly despite the presence of any native oxide on the micro-bumps. The values are acceptably low in the real industry and also comparable to those of the previous studies [12]–[15], [20]–[24]. Thus, it is expected that reliable results with low contact resistance will be obtained if the side contact is well conducted because of the similar values of the contact resistance of both the Cu pillar and the solder.

Since the probes were well manufactured and measured, we fabricated them in arrays to check the possibility for commercial realization in the industry. As shown in Fig. 12, about 10,000 units of probes were made uniformly in one area. However, we can see some impurities among the probe array in Fig. 12(a) and a bit of non-uniformity as distribution of the diameter of the contactors are described through Fig. 12(b)-(d). Also, we had experienced some probes bigger than usual at the edge of the probe arrays, called the edge effect, due to the current concentrating on the sharp edges during electroplating. This is a very commonly known issue that every electroplating environment needs to be optimized for every mold within consideration and knowhow. Therefore, our work with these issues of the fabrication can be fairly possible to be optimized in the near future. We expect that our new and simple technique realizes the probes contact to all the micro-bumps at once.

V. CONCLUSION

The conventional pre-bond testing method operates probes vertically on micro-bumps, and the contacted tip end of the micro-bumps inevitably gets damaged. This is detrimental to the IC assembly, which is the post-testing stage, because it causes a defective junction problem. To overcome this problem, we proposed lateral contact probing of fine pitch micro-bumps because it does not damage the tip end of the micro-bumps at all. We successfully demonstrated the testing, for the first time, with monolithically fabricated fine pitch probes. In addition, whereas conventional probes require a very complicated fabrication process for high flexibility to reduce the damage to the micro-bumps, another feature in this work is that the probes do not need high flexibility or complex fabrication. Thanks to the simple structure of the probes for the lateral contact, the fabrication is designed with only one thick negative PR mold and nickel electroplating to construct it all.

The fabricated probes were laterally driven as much as 7 μm without plastic deformation, which is acceptable considering the error in the plane direction of chips. In addition, the tested probes were repeatedly driven 5 μm for 100,000 cycles and their CCC was at least larger than 180 mA. With these probes, we successfully demonstrated contact without degradation on the tip end of the micro-bumps and the measured contact resistance was 1.13 Ω, the highest. All the side-walls of the micro-bumps showed low damage regardless of the material. Moreover, about 10,000 probes were uniformly fabricated in a batch process. By employing the proposed concepts with all the results we had, we expect this lateral contact probing method is a prospective solution for pre-bond testing of modern advanced fine-pitched micro-bumps.

REFERENCES

[1] (2015). *International Technology Roadmap for Semiconductors 2.0*. [Online]. Available: http://www.itrs2.net/itrs-reports.html
[2] R. S. Patti, "Three-dimensional integrated circuits and the future of system-on-chip designs," *Proc. IEEE*, vol. 94, no. 6, pp. 1214–1224, Jun. 2006.
[3] E. J. Marinissen, "Challenges and emerging solutions in testing TSV-based 2 1 over 2D- and 3D-stacked ICs," in *Proc. DATE*, Dresden, Germany, Mar. 2012, pp. 1277–1282.
[4] E. Beyne and B. Swinnen, "3D system integration technologies," in *Proc. IEEE Int. Conf. ICICDT*, Austin, TX, USA, May/Jun. 2007, pp. 1–3.
[5] E. J. Marinissen, "Testing TSV-based three-dimensional stacked ICs," in *Proc. DATE*, Dresden, Germany, Mar. 2010, pp. 1689–1694.
[6] J.-N. Ahn, "Fabrication of the micromachined monolithic micro-probe with rounded anchor," M.S. thesis, School Elect. Eng., KAIST, Daejeon, South Korea, 2006.
[7] R. Vallauri and E. J. Marinisse, "Challenges probing next generation full array products with 60 μm pitch and below," presented at the IEEE SWTW, 2015. [Online]. Available: http://www.technoprobe.com/press-news/publications/

[8] F. X. Reng, R. Vallauri, and C. Plotz, "AMD high pin count probing challenges on leading edge GPU: Technoprobe TPEGTM MEMS vs. cobra," presented at the IEEE SWTW, 2016. [Online]. Available: http://www.technoprobe.com/press-news/publications/

[9] E. J. Marinissen and Y. Zorian, "Testing 3D chips containing through-silicon vias," in *Proc. Int. Test Conf.*, Austin, TX, USA, Nov. 2009, pp. 1–11.

[10] B. Eldrige and M. Loranger, "Challenges and solutions for testing of TSV and micro-bump," in *IEEE Int. Workshop 3D-TEST Dig.*, Sep. 2011, p. 72.

[11] G. Böhm, S. Kalt, A. Klumpp, E. Marinissen, J. Kiesewetter, and W. Schäfer, "Very small pitch micro bump array probing," presented at the IEEE SWTW, 2013. [Online]. Available: http://www.swtest.org/swtw_library/2013proc/swtw2013.html

[12] O. Yaglioglu and B. Eldridge, "Direct connection and testing of TSV and microbump devices using NanoPierce contactor for 3D-IC integration," in *Proc. IEEE VLSI Test Symp.*, Hyatt Maui, HI, USA, Apr. 2012, pp. 96–101.

[13] O. Yaglioglu and B. Eldridge, "Contact testing of copper micro-pillars with very low damage for 3D IC assembly," in *Proc. IEEE Int. 3D Syst. Integr. Conf.*, San Francisco, CA, USA, Oct. 2013, pp. 1–4.

[14] T. Lai and C. Tsou, "A claw type of MEMS probe card for the electrical testing of micro-solder ball," in *Proc. IEEE MEMS*, Paris, France, Jan./Feb. 2012, pp. 345–348.

[15] C. Tsou, T. Lai, and C. Huang, "A novel micromachined claw probe for the electrical testing of microsolder ball," *J. Microelectromech. Syst.*, vol. 21, no. 5, pp. 1022–1031, Oct. 2012.

[16] R. Vettori, R. Vallauri, M. DiEgidio, and E. Bertarelli, "General overview on pad damage: Probe key parameters and other causes," presented at the IEEE SWTW, 2016. [Online]. Available: http://www.technoprobe.com/press-news/publications/

[17] R. Vallauri, "TPEGTM: A new vertical MEMS solution for high current, low pitch applications," presented at the IEEE SWTW, 2012. [Online]. Available: http://www.technoprobe.com/press-news/publications/

[18] E. C. C. Yeh, W. J. Choi, K. N. Tu, P. Elenius, and H. Balkan, "Current-crowding-induced electromigration failure in flip chip solder joints," *Appl. Phys. Lett.*, vol. 5, no. 4, pp. 580–582, Jan. 2002.

[19] W. J. Choi, E. C. C. Yeh, and K. N. Tu, "Mean-time-to-failure study of flip chip solder joints on Cu/Ni(V)/Al thin-film under-bump-metallization," *J. Appl. Phys.*, vol. 94, no. 9, pp. 5665–5671, Nov. 2003.

[20] K. Smith *et al.*, "Evaluation of TSV and micro-bump probing for wide I/O testing," in *Proc. Int. Test Conf.*, Anaheim, CA, USA, Sep. 2010, pp. 1–10.

[21] E. J. Marinissen, B. Wachter, K. Smith, J. Kiesewetter, M. Taouil, and S. Hamdioui, "Direct probing on large-array fine-pitch micro-bumps of a wide-I/O logic-memory interface," in *Proc. Int. Test Conf.*, Seattle, WA, USA, Oct. 2014, pp. 1–10.

[22] F. Wang *et al.*, "Two-dimensional dense-arrayed probe-cards with a hoe-shaped probing-tip micromachining technique," in *Proc. IEEE MEMS*, Wuhan, China, Jan. 2008, pp. 343–346.

[23] F. Wang, X. Li, and S. Feng, "A MEMS probe card with 2D dense-arrayed 'hoe'-shaped metal tips," *J. Micromech. Microeng.*, vol. 18, no. 5, p. 055008, Mar. 2008.

[24] F. Wang, R. Cheng, and X. Li, "MEMS vertical probe cards with ultra densely arrayed metal probes for wafer-level IC testing," *J. Microelectromech. Syst.*, vol. 18, no. 4, pp. 933–941, Oct. 2012.

[25] M. Losey, T. Hu, F. Cros, J. Andberg, and R. Smith, "A low-force MEMS probe solution for fine-pitch 3D-SIC wafer test," in *IEEE Int. Workshop 3D-TEST Dig.*, 2011, p. 73.

[26] J. Tang *et al.*, "An investigation of microstructure and mechanical properties of UV-LIGA nickel thin films electroplated in different electrolytes," *J. Micromech. Microeng.*, vol. 20, no. 2, p. 025033, Jan. 2010.

[27] A. M. Rashidi and A. Amadeh, "Effect of electroplating parameters on microstructure of nanocrystalline nickel coatings," *J. Mater. Sci. Technol.*, vol. 26, no. 1, pp. 82–86, Jan. 2010.

[28] I. Matsui, Y. Takigawa, T. Uesugi, and K. Higashi, "Enhanced tensile ductility in bulk nanocrystalline nickel electrodeposited by sulfamate bath," *Mater. Lett.*, vol. 65, nos. 15–16, pp. 2351–2353, Aug. 2011.

[29] K. P. Larsen, A. A. Rasmussen, J. T. Ravnkilde, M. Ginnerup, and O. Hansen, "MEMS device for bending test: Measurements of fatigue and creep of electroplated nickel," *Sens. Actuators A, Phys.*, vol. 103, nos. 1–2, pp. 156–164, Jan. 2003.

[30] H. S. Cho, K. J. Hemker, K. Lian, and J. Goettert, "Tensile, creep and fatigue properties of LIGA nickel structures," in *IEEE MEMS Tech. Dig.*, Las Vegas, NV, USA, Jan. 2002, pp. 439–442.

[31] H.-D. Kim, G.-W. Yoon, J.-H. Yeon, J.-H. Lee, and J.-B. Yoon, "Fabrication of a uniform microlens array over a large area using self-aligned diffuser lithography (SADL)," *J. Micromech. Microeng.*, vol. 22, no. 4, p. 045002, Mar. 2012.

[32] G. M. Rebeiz, *RF MEMS Theory, Design and Technology*, 1st ed. Hoboken, NJ, USA: Wiley, 2003.

[33] Y.-H. Song, D.-H. Choi, H.-H. Yang, and J.-B. Yoon, "An extremely low contact-resistance MEMS relay using meshed drain structure and soft insulating layer," *J. Microelectromech. Syst.*, vol. 20, no. 1, pp. 204–211, Feb. 2011.

[34] Y.-H. Yoon *et al.*, "A highly reliable MEMS relay with two-step spring system and heat sink insulator for high-power switching applications," *J. Microelectromech. Syst.*, vol. 25, no. 1, pp. 217–226, 2016.

[35] (2009). *ISMI Probe Council Current Carrying Capability Measurement Guideline, International SEMATECH Manufacturing Initiative*. [Online]. Available: http://www.sematech.org/docubase/document/5021atr.pdf

[36] R. Vallauri, D. Perego, M. Prea, J. Kim, and J. Yun, "HBM fine pitch micro pillar grid array probing evaluation," presented at the IEEE SWTW, 2017. [Online]. Available: http://www.swtest.org/swtw_library/2017proc/swtw2017.html

Chang-Keun Kim received the B.S. degree from the School of Electrical Engineering, Korea Advanced Institute of Science and Technology (KAIST), Daejeon, South Korea, in 2015, and the M.S. degree from KAIST in 2017. He spent most of the master's degree working on the development and fabrication of MEMS probe card technology for the simultaneous contact and probing of fine pitch micro-bumps. He is interested in computer science and is currently researching database management systems.

Yong-Hoon Yoon received the B.S. degree in material science and engineering from the University of Seoul, Seoul, South Korea, in 2012, and the M.S. and Ph.D. degrees in electrical engineering from the Korea Advanced Institute of Science and Technology, Daejeon, South Korea, in 2014 and 2018, respectively. During his M.S. and Ph.D. research, he was involved in MEMS switch for RF and power applications. He is currently an FBAR Filter Designer with Broadcom Ltd.

Donguk Kwon received the B.S., M.S., and Ph.D. degrees in mechanical engineering from the Korea Advanced Institute of Science and Technology, Daejeon, South Korea, in 2012, 2014, and 2018, respectively. He is currently a Researcher with Samsung Electronics Co., Ltd.

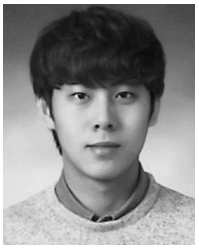

Seunghwan Kim received the B.S. degree in mechanical engineering from Sungkyunkwan University, South Korea, in 2014, and the M.S. degree in mechanical engineering from the Korea Advanced Institute of Science and Technology, South Korea, in 2016, where he is currently pursuing the Ph.D. degree. His research interests are flexible physical sensors, human-interface devices, electronic skin, and wearable devices.

Gun-Wook Yoon received the B.S. degree from the School of Electrical Engineering, Korea University, Seoul, South Korea, in 2010, and the M.S. degree from the School of Electrical Engineering, Korea Advanced Institute of Science and Technology, Daejeon, South Korea, in 2012, where he is currently pursuing the Ph.D. degree with the Department of Electrical Engineering. His current research interests are focused on micro-fabrication and display.

Min Woo Rhee was born in Seoul, South Korea, in 1973. He received the B.Eng. (Hons.), M.Sc., and the Ph.D. degrees in chemical engineering from Sogang University, Seoul, and the master's degree in management of technology from the National University of Singapore, Singapore. He has about 20 years' experience in microelectronics packaging research and development for both industry and research institutes. He also has extensive experience in new packaging and material development, modeling, and characterization. He was also with Amkor Technology Research and Development from 1999 to 2010, where he was the Senior Manager and the Leader of the Material Characterization Modeling and Failure Analysis Group. He also resolved lots of chronic failure and quality issues with worldwide semiconductor companies. He has been the Program Manager and a Principal Engineer with the Manufacturing Technology Research and Development Center, Samsung Electronics, Hwasung, South Korea, since 2015. Before joining Samsung Electronics, he was a Scientist and the Group Leader in interconnection and advanced packaging program with the Institute of Microelectronics (IME), Agency for Science, Technology and Research, Singapore. Moreover, he led power module, ruggedized electronics groups, and industry consortium projects for automotive, oil and gas, deep sea exploration, and aerospace industries. He also has project leading experience on lots of public funded and industry projects related to material and new packaging development, such as MEMs and 3-D-IC packaging during his working in IME from 2011 to 2015. Before joining IME, he had developed an automotive three-phase inverter module for power electronics with the Fairchild Semiconductor Research and Development Group as a Principal Engineer, which were successfully applied SiP products for mass production for automotive industries. Moreover, he received The Future Creator Award from Samsung Electronics in 2018 and the Best Employee of the Year Award when he was with Amkor in 2009.

Jinyeong Yun received the B.E. degree in control and instrumentation engineering and the M.E. degree in control engineering from Ajou University, Suwon, South Korea, in 1993 and 1995, respectively. He is currently a Principal Engineer with the Mechatronics Research and Development Center, Samsung Electronics, Hwasung, South Korea. During his 10 years of working at Samsung Electronics, he was involved in developing automatic test equipment for functional testing of semiconductor devices, such as DDI, CIS, RF card, flash memory, and DRAM. Since 2016, he has been developing a brand-new and world-first testing methodology and its equipment for high-bandwidth memory including 55-μm pitched micro pillar grid array probing.

Inkyu Park received the B.S. degree from the Korea Advanced Institute of Science and Technology (KAIST), Daejeon, South Korea, in 1998, the M.S. degree from the University of Illinois at Urbana–Champaign, USA, in 2003, and the Ph.D. degree from the University of California at Berkeley, Berkeley, USA, in 2007, all in mechanical engineering. He has been a Faculty Member with the Department of Mechanical Engineering, KAIST, since 2009, where he is currently an Associate Professor. He has published over 60 international journal articles (SCI indexed) and 100 international conference proceeding papers in the areas of MEMS/NANO engineering. His research interests are nanofabrication, smart sensors, nanomaterial-based sensors, and flexible and wearable electronics. He was a recipient of the IEEE NANO Best Paper Award (2010) and the HP Open Innovation Research Award (2009–2012).

Jun-Bo Yoon (S'92–A'99–M'01) received the B.S. *(summa cum laude)*, M.S., and Ph.D. degrees in electrical engineering from the Korea Advanced Institute of Science and Technology (KAIST), Daejeon, South Korea, in 1993, 1995, and 1999, respectively. During the Ph.D. research, he was involved in high-Q micromachined inductor, which was cited as the best work on planar inductors at that time in *Rf Mems: Theory, Design, And Technology* (Gabriel Rebeiz). From 1999 to 2000, he was with the University of Michigan, Ann Arbor, MI, USA, as a Post-Doctoral Research Fellow, where he invented the first movable-dielectric tunable RF MEMS capacitor, which holds the record for highest Q-factor. Since 2000, he has been with the Department of Electrical Engineering, KAIST, where he is currently a Professor. He was with Stanford University, Stanford, CA, USA, from 2008 to 2009, on his sabbatical leave. In 2017, he co-founded a startup company, MEMSLUX. He was involved in the MEMS fields for over 25 years. He has made contributions to the world's smallest/lowest-voltage nanoelectromechanical switches, the invention of 3-D diffuser lithography, and high-Q RF MEMS components. He has authored or co-authored over 200 journals and conference papers. He holds 41 international and 87 Korean patents. His research interests include nanowire-based physical/chemical sensors, RF/display MEMS, and micro/nanoelectromechanical switches. He was the Editor-in-Chief of the *Micro and Nano Systems Letters* from 2015 to 2017. He is currently an Editor of the IEEE JOURNAL OF MICROELECTROMECHANICAL SYSTEMS. He is on the Editorial Boards of the IOP *Journal of Micromechanics and Microengineering*.

Dr. Yoon has served as a Technical Program Committee Member of the IEEE A-SSCC 2007, Transducers 2009–2011, IEEE MEMS 2009–2010, IEEE MEMS 2017–2018, and IEEE IEDM 2017 conferences, and an Executive Program Committee Member of Transducers 2013–2015. He will be the Designated Co-General Chair of the MEMS 2019 Conference, Seoul, South Korea. He was a recipient of the Third-Place Award of the Student Paper Competition presented at the International Microwave Symposium, IEEE Microwave Theory and Techniques Society, in 1999. He received the Department Excellent Teaching Awards in 2003, 2007, 2011, and 2016, respectively, and the University Excellent Teaching Award in 2006.